

Article

Susceptibility of CoFeB/AIO_x/Co Magnetic Tunnel Junctions to Low-Frequency Alternating Current

Yuan-Tsung Chen * and Zu-Gao Chang

Department of Materials Science and Engineering, I-Shou University, Kaohsiung 840, Taiwan;
E-Mail: isu10107014m@cloud.isu.edu.tw

* Author to whom correspondence should be addressed; E-Mail: ytchen@isu.edu.tw;
Tel.: +886-765-777-11 (ext. 3119); Fax: +886-765-784-44.

Received: 21 August 2013; in revised form: 8 October 2013 / Accepted: 10 October 2013 /
Published: 15 October 2013

Abstract: This investigation studies CoFeB/AIO_x/Co magnetic tunneling junction (MTJ) in the magnetic field of a low-frequency alternating current, for various thicknesses of the barrier layer AIO_x. The low-frequency alternate-current magnetic susceptibility (χ_{ac}) and phase angle (θ) of the CoFeB/AIO_x/Co MTJ are determined using an χ_{ac} analyzer. The driving frequency ranges from 10 to 25,000 Hz. These multilayered MTJs are deposited on a silicon substrate using a DC and RF magnetron sputtering system. Barrier layer thicknesses are 22, 26, and 30 Å. The X-ray diffraction patterns (XRD) include a main peak at $2\theta = 44.7^\circ$ from hexagonal close-packed (HCP) Co with a highly (0002) textured structure, with AIO_x and CoFeB as amorphous phases. The full width at half maximum (FWHM) of the Co(0002) peak, decreases as the AIO_x thickness increases; revealing that the Co layer becomes more crystalline with increasing thickness. χ_{ac} result demonstrates that the optimal resonance frequency (f_{res}) that maximizes the χ_{ac} value is 500 Hz. As the frequency increases to 1000 Hz, the susceptibility decreases rapidly. However, when the frequency increases over 1000 Hz, the susceptibility sharply declines, and almost closes to zero. The experimental results reveal that the mean optimal susceptibility is 1.87 at an AIO_x barrier layer thickness of 30 Å because the Co(0002) texture induces magneto-anisotropy, which improves the indirect CoFeB and Co spin exchange-coupling strength and the χ_{ac} value. The results concerning magnetism indicate that the magnetic characteristics are related to the crystallinity of Co.

Keywords: magnetic tunnel junctions (MTJs); indirect exchange coupling; low-frequency alternate-current magnetic susceptibility (χ_{ac}); resonance frequency (f_{res})

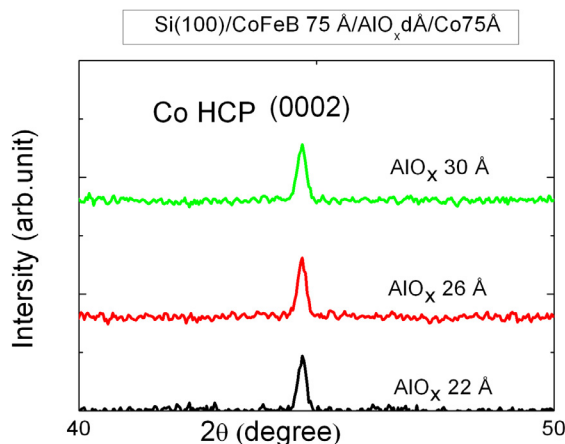
1. Introduction

Recently, ferromagnetic exchange-coupling in magnetic fields has been extensively examined. Exchange-coupling has been discussed following the discovery of spintronics [1–3]. Magnetic tunneling junctions (MTJs) have a sandwiched structure, which is composed of a top ferromagnetic (FM1) layer, an insulating tunneling layer (spacer), and a bottom ferromagnetic (FM2) layer, which can be utilized in high-density read/write heads, magnetoresistance random access memories (MRAM) and gauge sensor applications. This structure yields a very large magnetoresistance (MR) owing to spin-dependent tunneling effect [4–10]. Numerous factors influence the magnetoresistance, such as the indirect spin exchange-coupling of ferromagnetic layers, and the quality of the insulating tunneling layer, which affect the magnetic performance. The indirect exchange coupling between FM1 and FM2 layers in MTJs is interesting to investigate because the indirect exchange coupling can influence saturation magnetization (M_s) and coercivity (H_c) [11]. However, a high-quality MTJ must have superior ferromagnetic layers, a high spin-polarization, a microstructure that is as close to ideal as possible, and indirect spin exchange-coupling between the FM1 and FM2 ferromagnetic layers. However, most MTJ research has focused on tunneling magnetoresistance (TMR). Additionally, most relevant investigations of magnetism have focused on high-frequency magnetic impedance (MI) [12]. Only a few have focused on low-frequency alternate-current magnetic susceptibility (χ_{ac}) and the optimal resonance frequency (f_{res}). Susceptibility to low-frequency alternate-current magnetism and the effect of the thickness of the tunneling barrier on indirect exchange coupling between FM1 and FM2 in the CoFeB/ AlO_x /Co junction are worthy of study. In this study, the thickness of CoFeB and Co is 75 Å and the AlO_x barrier thickness is varied among 22, 26, and 30 Å. The X-ray diffraction patterns (XRD) includes a hexagonal close-packed (HCP) Co(0002)-textured structure at $2\theta = 44.7^\circ$, and AlO_x and CoFeB are amorphous phases. The results concerning χ_{ac} reveal that the susceptibility distribution is optimal at low frequency. The three highest values of susceptibility for each sample are averaged. When the thickness of the AlO_x barrier is 30 Å, the mean susceptibility is highest, at 1.87, it is lowest, 1.19, at a barrier thickness of 22 Å. In summary, the susceptibility was very sensitive to variable AlO_x barrier thickness. The susceptibility results demonstrate that the magnetic characteristics are related to the Co crystallinity and the thickness of the AlO_x barriers.

2. Results and Discussion

Figure 1 presents the XRD patterns of the laminated CoFeB(75 Å)/ $\text{AlO}_x(d)$ /Co(75 Å) MTJ junctions. They reveal that the junctions have a hexagonal close-packed (HCP) Co(0002) texture at $2\theta = 44.7^\circ$. The microstructures of CoFeB and AlO_x are amorphous. According to previous references [13,14], we can also reasonably conclude that the diffracted peak is Co(0002). Therefore, the HCP Co(0002) was identified herein.

Figure 1. X-ray diffraction patterns of CoFeB(75 Å)/AlO_x(*d* Å)/Co(75 Å) magnetic tunneling junction (MTJ).



The full width at half maximum (FWHM, B) of the Co(0002) peak as a function of AlO_x thickness was extracted from a mathematical fit to the data, which is shown in Figure 2. Scherrer's formula can be written as:

$$D = 0.9\lambda/B \cos\theta \quad (1)$$

where D represents the grain size; λ is the wavelength of the CuK_{α1} line; B is the full width at half maximum of the (0002) peak and θ is the half angle of the diffraction peak. This formula can be applied to calculate the grain size and determine the crystallinity [15]. From Figure 2, B is reduced by increasing the AlO_x tunnel barrier thickness, reducing the FWHM of the peak of the Co layer. This phenomenon explains that the small B can induce the increase in the grain size of Co and the enhancement of the Co(0002) texture. In the deposited structure, the thickness and crystallinity of seed layer play an important parameter to providing the crystallinity of top layer [16]. In this study, it suggests that the AlO_x thickness is related to grain size and crystallinity of Co layer. Moreover, the related study also indicates that the AlO_x thickness of MTJ can affect Co structure, grain size, and exchange coupling strength [11]. The magneto crystalline anisotropy of Co(0002) texture can enhance its magnetic properties [17].

Figure 2. Full width at half maximum (FWHM) (B) as a function of thickness (d) of AlO_x layer.

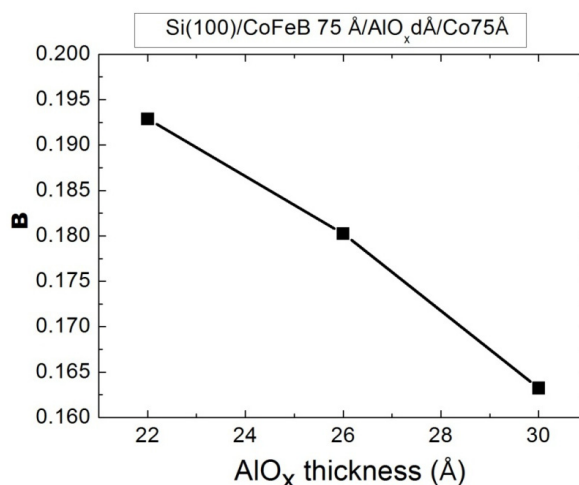
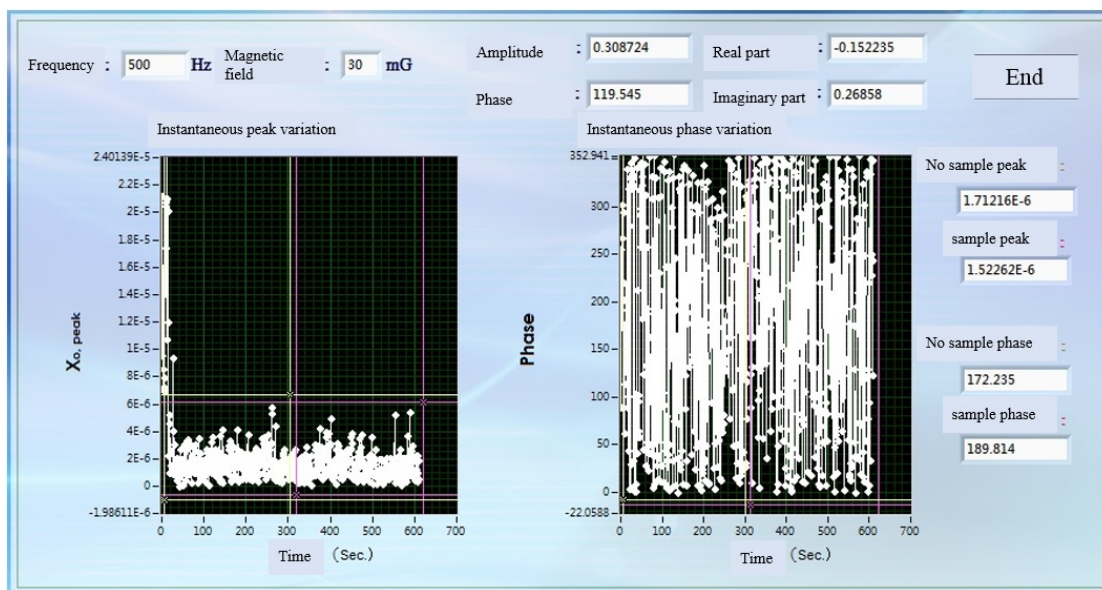
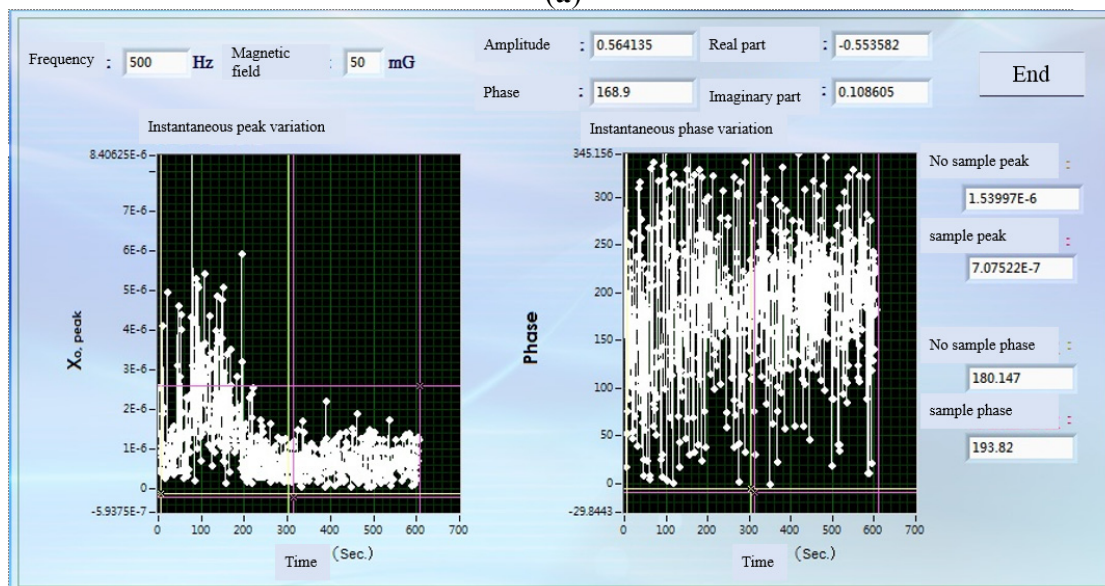


Figure 3 shows the different magnitude and direction of the external magnetic field are provided in χ_{ac} measurement. According to the result, the in-plane χ_{ac} signal of MTJ is larger than the perpendicular χ_{ac} signal. It indicates that in-plane direction is easy-axis magnetization of MTJ.

Figure 3. (a) The perpendicular χ_{ac} signal of MTJ sample when the external field is 30 mOe; (b) The perpendicular χ_{ac} signal of MTJ sample when the external field is 50 mOe; (c) The in-plane χ_{ac} signal of MTJ sample when the external field is 30 mOe; (d) The in-plane χ_{ac} signal of MTJ sample when the external field is 50 mOe.

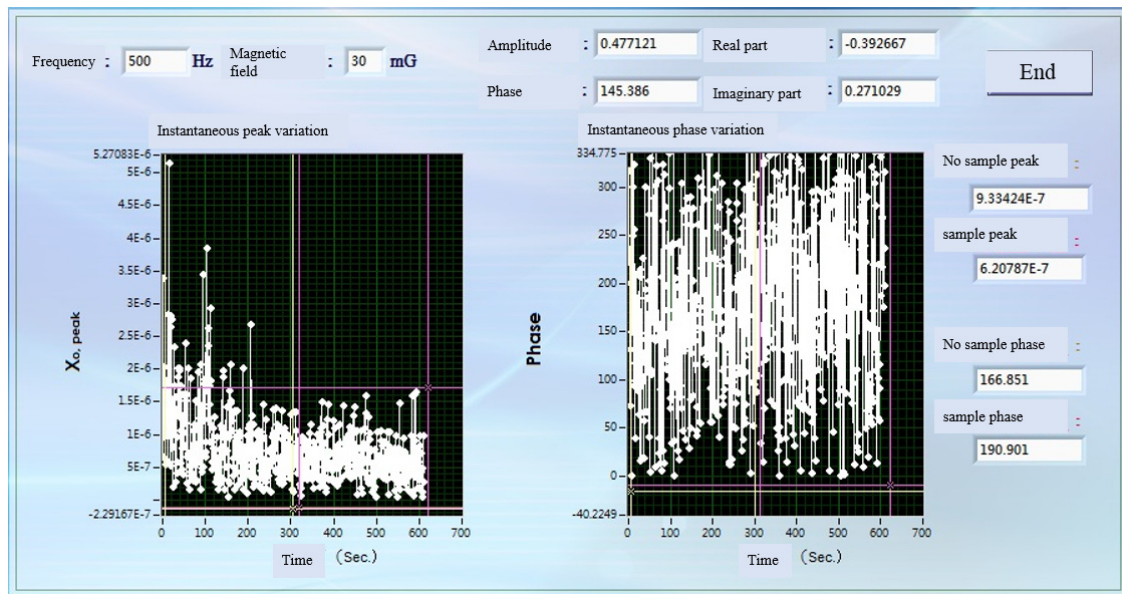


(a)

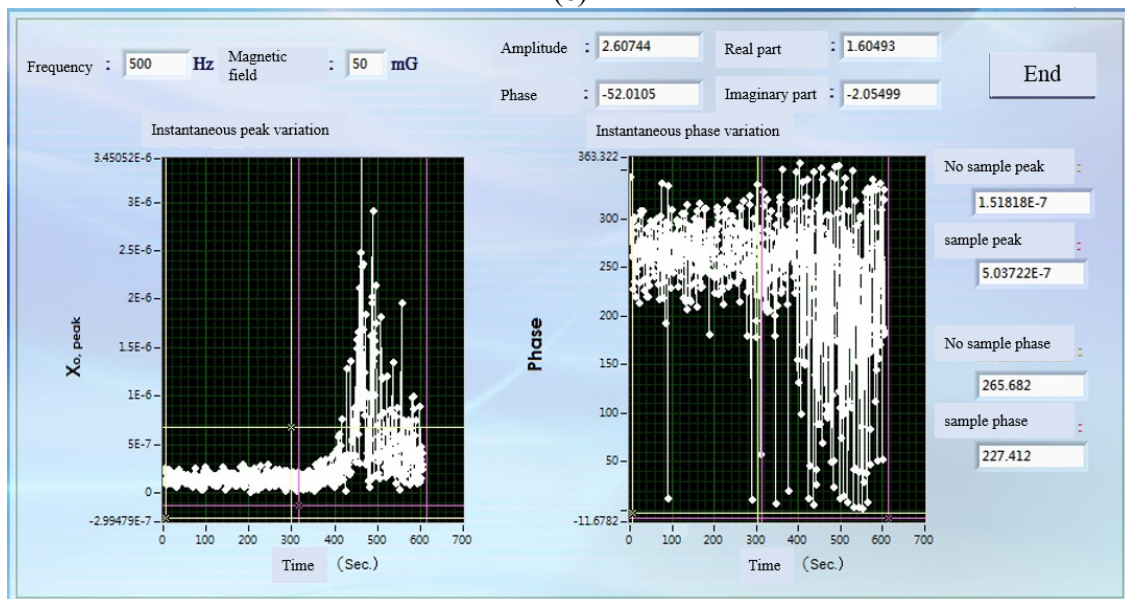


(b)

Figure 3. Cont.



(c)



(d)

Figure 4 shows the low-frequency alternate-current magnetic susceptibility (χ_{ac}) of the multilayered CoFeB/ AlO_x /Co with AlO_x barrier thicknesses of 22, 26 and 30 Å and a variable frequency from 10 to 25,000 Hz. The χ_{ac} has the following physical meaning. The magnetic material under the external AC magnetic field shows a magnetic property called multiple-frequency AC magnetic susceptibility χ_{ac} . The origin of χ_{ac} is due to the association between magnetic spin interactions. The frequency of the applied AC magnetic field equals the frequency of oscillation of the magnetic dipole. Hence, the frequency of the peak of the low-frequency magnetic susceptibility corresponds to the resonant frequency of the oscillation of the magnetic dipole moment inside domains. The χ_{ac} peak indicates the spin exchange-coupling interaction and dipole moment of domain under frequency [18]. It is reasonably concluded that the physical meaning peaks of the low frequency susceptibility indicate the magnetic exchange coupling between CoFeB and Co layers. The susceptibility peaks relate to the

exchange interaction between CoFeB and Co layers closely. The high χ_{ac} peaks are corresponding to high exchange coupling. From Figure 4, the optimal susceptibility was obtained at the optimal resonance frequency (f_{res}) of 500 Hz for independently of AlO_x barrier thickness. It indicates that the optimal exchange-coupling strength of MTJ occurs at 500 Hz. The maximum χ_{ac} corresponds to the maximum spin sensitivity at f_{res} . Additionally, the susceptibility of the films sharply fell to zero as the frequency was increased over 1000 Hz. The MTJ with a AlO_x thickness of 30 Å had the highest χ_{ac} of approximately 1.87 at a f_{res} of 500 Hz because Co(0002) texture induces a magneto nanocrystalline anisotropy with the maximum χ_{ac} and f_{res} effect [17]. From this result, multilayered MTJs are reasonably inferred to be ideal for use in low-frequency sensors and transformers. Moreover, for mechanical components, the optimal condition is suitable in each MTJ, because the optimal resonance frequency of 500 Hz is stable.

Figure 4. Susceptibility (χ_{ac}) of CoFeB/ AlO_x ($d = 22, 26$ and 30 Å)/Co MTJs as a function of frequency, 10–25,000 Hz.

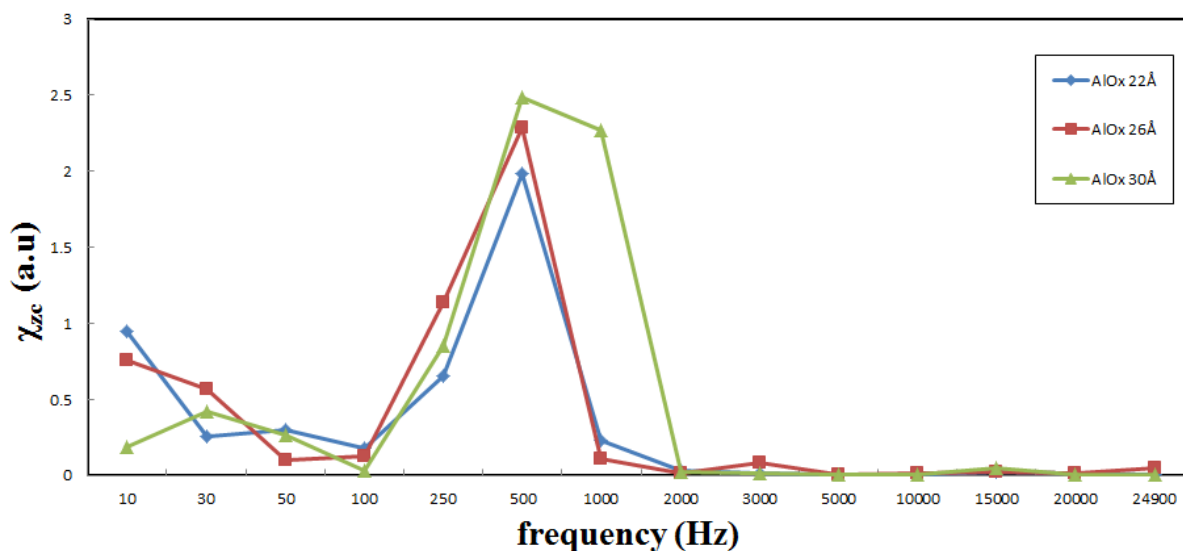


Figure 5 plots the mean optimal susceptibility and phase angle for AlO_x barriers with thicknesses of 22, 26, and 30 Å. The average phase angle corresponds to the mean optimal susceptibility. It is 49.07° , 94.94° , and 156.71° , at thicknesses of 22, 26, and 30 Å, respectively. From Table 1 and Figure 5, the mean optimal susceptibility increases from 1.19 to 1.87 as the average phase angle varies from 49.07° to 156.71° . The mean maximum χ_{ac} and phase angle increase with the AlO_x barrier thickness because the magneto-anisotropy of Co(0002) texture induces strong indirect spin exchange coupling between CoFeB and Co, increasing χ_{ac} . The results in Figure 5 also indicate that χ_{ac} increases with the phase angle. The χ_{ac} and the phase angle follow vary similarly. Moreover, an increasing phase angle is associated with increasingly sensitive to spin exchange-coupling strength, which is observed as a high susceptibility.

Figure 5. Mean optimal susceptibility and average phase angle as functions of AlO_x barrier thickness.

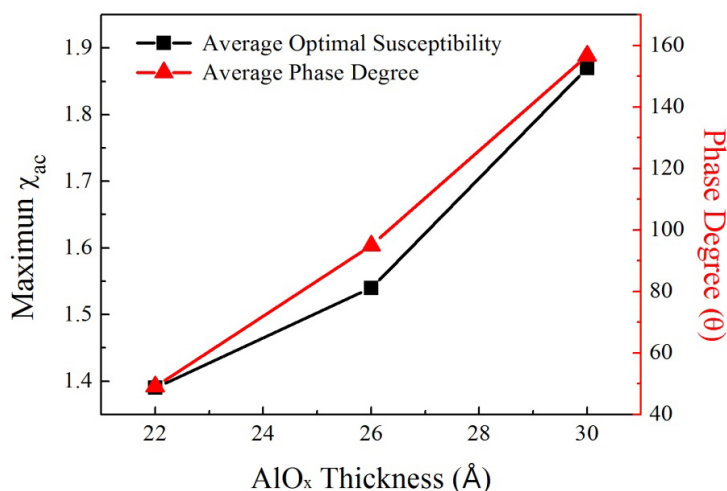


Table 1. High optimal susceptibility, average optimal susceptibility, and resonance frequency of maximum mean susceptibility.

d (Å)	Optimal susceptibility No. 1	Optimal susceptibility No. 2	Optimal susceptibility No. 3	Average optimal susceptibility	Optimal resonance frequency
22	1.9861	0.9452	0.6536	1.1950	500 Hz
26	2.2841	1.1405	0.7594	1.3947	500 Hz
30	2.4905	2.2711	0.8487	1.8700	500 Hz

3. Experimental Section

A multilayered MTJ was deposited on a Si(100) substrate by DC and RF magnetron sputtering. The typical base chamber pressure was less than 2×10^{-7} Torr, and the Ar working chamber pressure was 5×10^{-3} Torr. The MTJs had the structure Si(100)/CoFeB(75 Å)/ $\text{AlO}_x(d)$ /Co(75 Å) with $d = 22, 26$ and 30 Å. The target composition of the CoFeB alloy was 40 at.% Co, 40 at.% Fe, and 20 at.% B. To form an AlO_x barrier, Al was firstly deposited on the bottom FM electrode CoFeB layer, and the AlO_x layer was then formed by reactive sputtering in an oxidizing atmosphere that comprised a mixture of Ar/O₂ in the ratio 9:16. The plasma oxidation time varied from 50 to 70 s as the initial thickness of the Al layer increased from 22 to 30 Å. To examine the microstructure, the degree of Co(0002) layer texturing was characterized by X-ray diffraction (XRD) using $\text{CuK}\alpha_1$ radiation. The in-plane low-frequency alternate-current magnetic susceptibility (χ_{ac}) of MTJ was investigated using an χ_{ac} analyzer (XacQuan, MagQu Co. Ltd., Sindian City, Taiwan). About the χ_{ac} measurement, the referenced standard sample is calibrated by χ_{ac} analyzer with an external field. The size of standard sample is 5 mm × 5 mm. After the calibration is finish, the same size MTJ is placed in χ_{ac} measurement. The driving frequency ranged from 10 to 25,000 Hz. The χ_{ac} is determined through the magnetization measurement. All measured samples had the same shape and size to eliminate the demagnetization factor. The χ_{ac} value is unitless, because the χ_{ac} result is corresponding to referenced standard sample.

4. Conclusions

The CoFeB/ AlO_x /Co multilayer film is used to investigate the strength of indirect spin exchange-coupling between CoFeB and Co strength and the magnetic property χ_{ac} , in a low-frequency alternating magnetic field, for various thicknesses of the barrier layer AlO_x . The X-ray diffraction patterns include a main peak from highly (0002)-textured hexagonal close-packed (HCP) Co; AlO_x and CoFeB are amorphous phases. The full width at half maximum (FWHM) of the Co(0002) peak decreases as the AlO_x thickness increases, indicating that the Co layer becomes more crystalline. The results concerning the magnetism of all film samples demonstrate that the maximum χ_{ac} value is obtained at the optimal f_{res} of 500 Hz. As the frequency increased further to 1000 Hz, the susceptibility rapidly declined. Beyond 1000 Hz, it decreased sharply, almost to zero. As the barrier layer thickness increased, the χ_{ac} and phase angle increased because the magneto-anisotropy of the Co(0002) texture induced strong indirect spin exchange coupling between CoFeB and Co, increasing χ_{ac} . Finally, the average optimal susceptibility of CoFeB(75 Å)/ AlO_x (30 Å)/Co(75 Å) reached 1.87. The susceptibility results indicate that the magnetic characteristics are related to the Co crystallinity and the thickness of the AlO_x barrier. These multilayered MTJs have a high susceptibility in a low-frequency alternate-current magnetic field, making them favorable for use in low-frequency storage drives and magnetic recording media.

Acknowledgments

This work was supported by the National Science Council, under Grant No. NSC100-2112-M-214-001-MY3.

Conflicts of Interest

The authors declare no conflict of interest.

References

1. Hoffmann, F.; Stankoff, A.; Pascard, H. Evidence for an exchange coupling at the interface between two ferromagnetic films. *J. Appl. Phys.* **2009**, *41*, 1022–1023.
2. Mauri, D.; Siegmann, H.C.; Bagus, P.S.; Kay, E. Simple model for thin ferromagnetic films exchange coupled to an antiferromagnetic substrate. *J. Appl. Phys.* **2009**, *62*, 3047–3049.
3. Heinrich, B.; Tserkovnyak, Y.; Woltersdorf, G.; Brataas, A.; Urban, R.; Bauer, G.E.W. Dynamic exchange coupling in magnetic bilayers. *Phys. Rev. Lett.* **2003**, *90*, 187601–187604.
4. Chen, Y.T.; Jen, S.U.; Yao, Y.D.; Wu, J.M.; Sun, A.C. Interfacial effects on magnetostriction of CoFeB/ AlO_x /Co junction. *Appl. Phys. Lett.* **2006**, *88*, 222509:1–222509:3.
5. Wang, D.; Nordman, C.; Daughton, J.; Qian, Z.; Fink, J. 70% TMR at room temperature for SDT sandwich junctions with CoFeB as free and reference layers. *IEEE Trans. Magn.* **2004**, *40*, 2269–2271.
6. Meng, H.; Lum, W.H.; Sbiaa, R.; Lua, S.Y.H.; Tan, H.K. Annealing effects on CoFeB-MgO magnetic tunnel junctions with perpendicular anisotropy. *J. Appl. Phys.* **2011**, *110*, 039904:1–039904:4.

7. Moriyama, T.; Ni, C.; Wang, W.G.; Zhang, X.; Xiao, J.Q. Tunneling magnetoresistance in (001)-oriented FeCo/MgO/FeCo magnetic tunneling junctions grown by sputtering deposition. *Appl. Phys. Lett.* **2006**, *88*, 222503:1–222503:3.
8. Wu, K.M.; Wang, Y.H.; Chen, W.C.; Yang, S.Y.; Shen, K.H.; Kao, M.J.; Tsai, M.J.; Kuo, C.Y.; Wu, J.C.; Horng, L. Repair effect on patterned CoFeB-based magnetic tunneling junction using rapid thermal annealing. *J. Magn. Magn. Mater.* **2007**, *310*, 1920–1922.
9. Djayaprawira, D.D.; Tsunekawa, K.; Nagai, M.; Maehara, H.; Yamagata, S.; Watanabe, N.; Yuasa, S.; Suzuki, Y.; Ando, K. 230% room-temperature magnetoresistance in CoFeB/MgO/CoFeB magnetic tunnel junctions. *Appl. Phys. Lett.* **2005**, *86*, 092502:1–092502:3.
10. Hayakawa, J.; Ikeda, S.; Lee, Y.M.; Matsukura, F.; Ohno, H. Effect of high annealing temperature on giant tunnel magnetoresistance ratio of CoFeB/MgO/CoFeB magnetic tunnel junctions. *Appl. Phys. Lett.* **2006**, *89*, 232510:1–232510:3.
11. Chen, Y.T.; Wu, J.W. Effect of tunneling barrier as spacer on exchange coupling of CoFeB/ AlO_x /Co trilayer structures. *J. Alloys Compd.* **2011**, *509*, 9246–9248.
12. Coïsson, M.; Tiberto, P.; Vinai, F.; Tyagi, P.V.; Modak, S.S.; Kane, S.N. Penetration depth and magnetic permeability calculations on GMI effect and comparison with measurements on CoFeB alloys. *J. Magn. Magn. Mater.* **2008**, *320*, 510–514.
13. Yang, J.J.; Ji, G.X.; Yang, Y.; Xiang, H.; Chang, Y.A. Epitaxial growth and surface roughness control of ferromagnetic thin films on Si by sputter deposition. *J. Electron. Mater.* **2008**, *37*, 355–360.
14. Kharmouche, A.; Cherif, S.M.; Bourzami, A.; Layadi, A.; Schmerber, G. Structural and magnetic properties of evaporated Co/Si(100) and Co/glass thin films. *J. Phys. D* **2004**, *37*, 2583–2587.
15. Chen, Y.T.; Chang, C.C. Effect of grain size on magnetic and nanomechanical properties of $\text{Co}_{60}\text{Fe}_{20}\text{B}_{20}$ thin films. *J. Alloys Compd.* **2010**, *498*, 113–117.
16. Roy, A.G.; Laughlin, D.E. Effect of seed layers in improving the crystallographic texture of CoCrPt perpendicular recording media. *J. Appl. Phys.* **2002**, *91*, 8076–8078.
17. Chen, Y.T.; Chang, Z.G. Low-frequency alternative-current magnetic susceptibility of amorphous and nanocrystalline $\text{Co}_{60}\text{Fe}_{20}\text{B}_{20}$ films. *J. Magn. Magn. Mater.* **2012**, *324*, 2224–2226.
18. Yang, S.Y.; Chien, J.J.; Wang, W.C.; Yu, C.Y.; Hing, N.S.; Hong, H.E.; Hong, C.Y.; Yang, H.C.; Chang, C.F.; Lin, H.Y. Magnetic nanoparticles for high-sensitivity detection on nucleic acids via superconducting-quantum-interference-device-based immunomagnetic reduction assay. *J. Magn. Magn. Mater.* **2011**, *323*, 681–685.